

LESSONS LEARNED FROM SPACE-SI EXPERIMENTS ON PRISMA MISSION

**Drago Matko⁽¹⁾, Tomaž Rodič^(1,3), Sašo Blažič^(1,2), Aleš Marsetič^(1,4),
Robin Larsson⁽⁵⁾, Eric Clacey⁽⁵⁾, Thomas Karlsson⁽⁵⁾, Krištof Oštir^(1,4), Gašper
Mušič^(1,2), Luka Teslić⁽¹⁾, and Gregor Klančar^(1,2)**

⁽¹⁾SPACE-SI, Aškerčeva 12, 1000 Ljubljana, Slovenia,
+38614768252, drago.matko@space.si

⁽²⁾University of Ljubljana, Faculty of Electrical Engineering,
Tržaška 25, 1000 Ljubljana, Slovenia, +38614768763, saso.blazic@fe.uni-lj.si

⁽³⁾University of Ljubljana, Faculty of Natural Sciences and Engineering,
Aškerčeva 12, 1000 Ljubljana, Slovenia, tomaz.rodic@space.si

⁽⁴⁾Scientific Research Centre of the Slovenian Academy of Sciences and Arts,
Novi trg 2, 1000 Ljubljana, Slovenia, +38614706100, kristof@zrc-sazu.si

⁽⁵⁾OHB Sweden AB, Solna strandväg 86, 171 22 Solna, Sweden,
+4686276440, robin.larsson@ohb-sweden.se

Abstract: *In the paper several lessons learned from the set of formation flying experiments, performed by the Slovenian Centre of Excellence for Space Sciences and Technologies (Space-SI) and OHB Sweden with Prisma Mango (for Main) and Tango (for Target) satellites in September 2011, are reviewed. First experiment performed was In-flight simulated radar interferometry where one satellite simulated SAR transmitter and receiver, and the other receiver only. Second experiment was the Observation of non-co-operative objects - space debris. On the basis of the space debris Two Line Elements, Mango was reoriented to point the Mango's vision based camera towards the point of closest approach and several images were taken in a sequence. A challenging task is the close observation of the space debris. In our experiment Tango was simulating the debris and its 3D model was reconstructed from the shots taken by Mango. Next lesson was learned from the In-flight simulated distributed instrument where Tango was acting as the holder of the optical system with lenses and/or mirrors while Mango was acting as the holder of detectors. The last but not the least lesson learned from the experiments was acquired from the critical evaluation of formation flying models.*

Keywords: *Formation flying guidance, Radar interferometry, Distributed instrument, Space debris, Formation flying models.*

1. Introduction

In Slovenia a new Centre of Excellence for Space Sciences and Technologies SPACE-SI has been established in 2010 with the main focus on small satellite technologies. The Research & Technical Development (RTD) goals of the SPACE-SI consortium consisting of academic institutions, high-tech SMEs and large industrial and insurance companies are focused on nano and micro satellite technologies that are enabling high precision interactive remote sensing and precise manoeuvring of small spacecrafts in formation flying missions.

To investigate newly emerging formation flying technology SPACE-SI and OHB Sweden performed a set of formation flying experiments in September 2011 with Prisma [1, 2, 3, 4] satellites Mango and Tango that were launched into a sun synchronous orbit with 725 km altitude and 06.00 h ascending node in June 2010. In the SPACE-SI formation flying experiments the critical manoeuvres for three types of missions were investigated with respect to the in-orbit performances. In the paper several lessons, learned from this set of formation flying experiments, are reviewed.

The paper is organized as follows: In Section 2 the In flight simulated radar interferometry remote sensing is described. In this experiment one satellite was simulated as the SAR transmitter and receiver, while the other was simulated as receiver only. Mango and Tango were flown one behind the other (along-track) separated by a distance of approximately 200 m for three consecutive orbits. The experiment Observation of non-co-operative objects is presented in Section 3. Two sub-experiments were performed to simulate the required procedures: Orbit identification and Close observation during Mangos's closest flight (5 m) and during its encircling of Tango (which simulated the debris) respectively, in order to make a 3D model of the observed object. Section 4 presents the In flight simulated distributed instrument remote sensing experiment, where Tango was simulating the holder of the optical system with lenses and/or mirrors and Mango the detectors (sensors). This experiment, where satellites were flying close to each other and parallel, was performed in two different versions: with in-track or with radial and cross-track displacement. Section 4 outlines formation models, including an extension of the Hill-Clohessy-Wiltshire (HCW) model to orbits with small eccentricity, derived by the method of small perturbation. All models are critically evaluated against the Prisma experiment and the lesson learned is presented.

2. In Flight Simulated Radar Interferometry Remote Sensing

Formation flying capabilities are especially important for satellite based interferometry using a synthetic aperture radar (Interferometric Synthetic Aperture Radar - InSAR). Because the phase angle of the backscattered signal for a given pixel is available, and phase is easily measured, it is possible to compare the phase differences of two different images of the same region and, from that comparison, find the relative locations of pixels in three dimensions [5]. The interferometry is using radar images, made from slightly different positions, i.e. from different orbits. By comparing the phase (Φ , and the phase difference $\Delta\Phi$) of a pair of images the height of the reflection and the shape of the surface (digital elevation model, DEM) can be determined. Depending on the imaging configuration, also surface changes (i.e. displacements, movements) can be observed.

Along-track synthetic aperture radar interferometry is currently not used widely since the only system capable of providing it is the German TanDEM-X constellation, developed by DLR, EADS Astrium in Infoterra [6,7]. It however offers entirely new opportunities; this application uses two separate radar antennas arranged longitudinally along the direction of flight; a method that permits the measurement of the speed of moving

objects, as the two satellites image the same area successively, with a brief interval in between. The method is particularly useful in oceanography, glaciology, and traffic research [8, 9]. For successful determination of speed measurements an optimal distance between the satellites (baseline) has to be used and maintained. It has been proven that the baseline should be between hundred and several hundred meters [5].

2.1. The experiment

The goal of the experiment was to evaluate whether the stability of a non-controlled formation can satisfy the requirements of the InSAR procedure. Mango and Tango were flying one behind the other (along-track) separated by a distance of approximately 200 m for three consecutive orbits. Only natural forces have influenced the relative position of the satellites, there was no thruster control. In order to evaluate the stability of the orbit, we have observed the absolute and relative position of both satellites. Observing Figure 1, presenting the along-track geometry simulated by STK [10] and the relative distance between the Tango and Mango satellites, one can see that the relative distance of the satellites has been slowly changing in all three directions, with maximums reaching almost 4 m. As expected due to relative orbit dynamics the position was more stable in the cross-track and radial directions, where the standard deviations are 0.36 m and 0.69 m respectively; the along-track distance has been changing up to several meters with the standard deviation of 1.77 m. During a typical image acquisition time the changes are much smaller - the orbit drifts are up to 3 cm. This is in the range of relative orbit determination accuracy, presumably to 2 cm in relative position and 0.5 m for the absolute position. The changes in the distances have been rather slow, reaching up to approximately 5 mm/s with the acceleration as low as 0.01 mm/s².

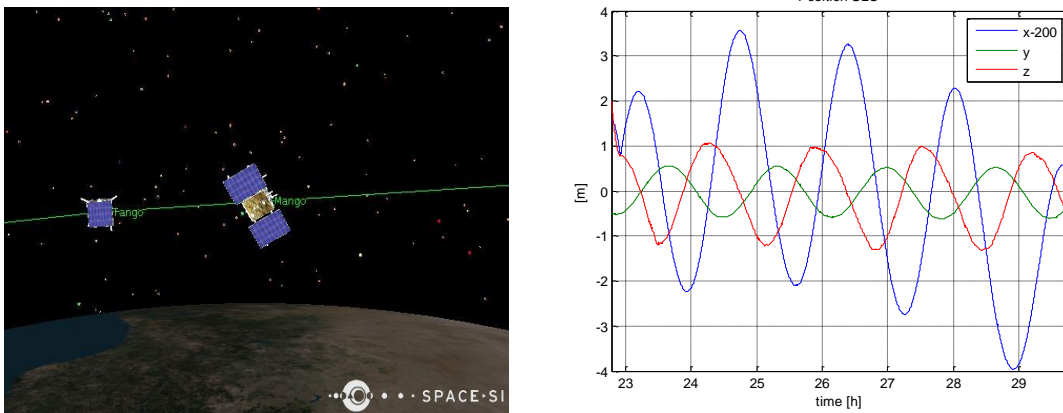


Figure 1. Along-track interferometric geometry STK simulation (left) and Relative distance between the Tango and Mango satellites (right).

2.2. Lessons learned

Since small drifts can be detected and corrected in InSAR processing, the Prisma constellation flight has proved to have the stability that is required for interferometric data processing [11]. All the drifting effects are small and removable during the InSAR

processing steps. The orbital stability and accuracy influences the estimated accuracy of velocity measurements obtained with along track interferometry. We have estimated that the measurement of water current speeds accuracy can reach 0.05 m/s. In a similar across-track constellation with similar orbital parameters and orbital accuracy the vertical accuracy of the digital elevation model production could reach 1 m.

3. Observation of Non-Co-Operative Objects

The non-co-operative objects such as space debris are and will become a serious problem since their orbits often overlap with trajectories of operational spacecraft, and represent a potential collision risk. In order to remove them, they must be identified. Two experiments were performed to simulate the required procedures, orbit identification and close observation.

3.1. Orbit identification

On the basis of the space debris Two Line Elements (TLE), Mango was reoriented to point the vision based camera (VBS camera with 14° field of view) towards the point of closest approach and several images were taken in a sequence. The criteria for choosing the object to be observed, was the distance and the duration of the close approach. Also additional constraints were considered: during imaging the camera should be pointing neither towards the Sun nor towards the Earth. Finally the satellite Geosat with ID number 15595, launched 1985, was chosen for observation. During observation just one minute before closest approach the debris of the Soviet Tsyklon rocket booster SL-14 R/B with ID number 22237 was flying in the field of view of the VBS camera. In the Figure 2 the sequence of taken pictures and corresponding STK animations are presented. The left three pictures show the close approach of the SL-14 R/B, which is in the STK animations (upper row) depicted in pink and is moving from right to left. In the VBS taken pictures (lower row) it can be seen as a white dot; a red arrow is pointing it for clarity reasons. The right three pictures show the close approach of the Geosat satellite.

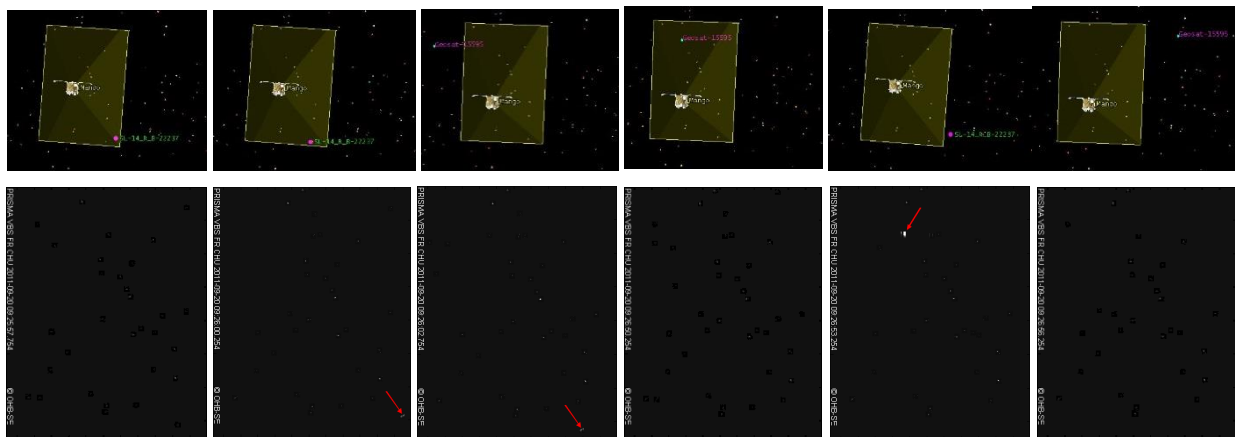


Figure 2. STK simulation (upper) and real camera shots (lower)

3.1. Close observation

A different and challenging task regarding space debris is close observation. In SPACE-SI's experiment this was performed in three different ways: First the satellites were flying in-track with a distance of 5 m. Mango was pointing its Digital Video System (DVS) camera towards Tango, which was acting as rotating space debris. The second observation took place while Mango was encircling Tango on an ellipse in the orbital plane while Tango was flying in its standard orientation (fixed in LVLH frame). Finally an appropriate cross-track movement was implemented to Mango in order to encircle Tango on a circular relative orbit with a radius of 20m for the third observation. A 3D model of Tango was reconstructed. A second objective of the close formation flying was to phase the natural motion around Tango such that images of predefined locations (Kuwait, Djibouti, Crete) on Earth could be captured with Tango in the foreground. Here the timing of images was precisely calculated in order to capture both targets simultaneously.

Immediately after the in-flight simulated distributed instrument remote sensing experiment (Section 4), the satellites were flown in the (in-track) distance of 5 m. This were ideal conditions for performing the close observation experiment with the satellites preserved in the same constellation, except for Mango pointing with its Digital Video System (DVS) camera towards Tango, which was rotating around (with a bit of wobbling) its cross-track axis, pointing all times with its solar panels toward the sun. Several pictures of Tango (which simulated the debris) were taken in order to make a 3D model of the observed object. Because of the non-optimal view angles and light conditions the 3D model was generated with manually selected tie points on the pictures. With tie points connecting the picture features (mainly satellite corners) the model was resolved and subsequently all model surfaces were added. At the end the textures were overlaid on the model surface. The left three images of the Figure 3 show the shots taken with the DVS camera (upper row) and corresponding views of the reconstructed 3D model (lower row). The corresponding solar panel front view of the 3D model was unsatisfactory since due to the Tango energy constraint, there was no corresponding shot by the DVS camera.

In order to have diversified images, an encircling of Tango by Mango in the orbit plane and in a relative 60 degrees inclined orbit on a circle with a radius of 20 m was also performed. Corresponding DVS shots and images of the reconstructed object (with far less details) are shown in the right two pictures of Figure 3 for the front and back side of the satellite respectively.

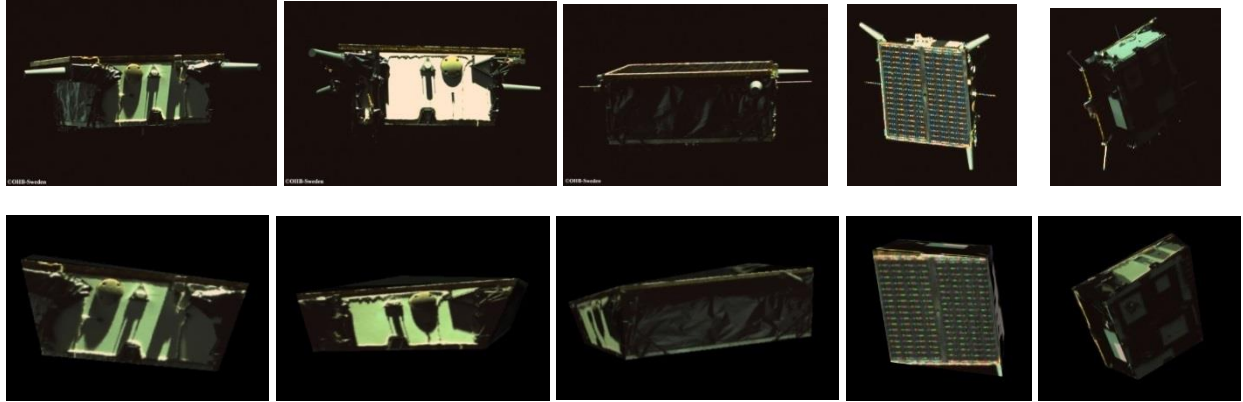


Figure 3. Picture shots of the DVS camera (upper) and the 3D model (lower), distance 5m (left three) and 20 m (right two)

The timing of imaging (during encircling) was adjusted to have some areas of interest on the surface of the Earth (Kuwait, Djibouti, Crete) in the background, as shown in Figure 4, where the left first and third picture represent the STK simulations using measured flight data (position and attitude), while the second from left and the most-right pictures show the corresponding Mango's DVS camera shots.



Fig. 4. The STK simulated and real (DVS) shot of the of the Persian Gulf (left two pictures) and Bab-el-Mandeb strait (right two pictures)

3.2. Lessons learned

The main lesson learned is that it is possible to predict close encounter between two satellites (including debris) from the TLE data. The second lesson learned from the close observation experiment is, that the reconstruction can be done successfully under satisfactory illumination conditions. However, such conditions are very hard to be met. The 3D model, reconstructed from the DVS camera shots with adequate resolution (from 5 m distance) is satisfactory, while the reconstruction of the parts reconstructed from a lower resolution images (taken from the 20 m distance), was degraded.

4. In-flight Simulated Distributed Instrument Remote Sensing

Precise formation flying of small satellites can also lead to interesting scenarios for optical remote sensing. One of them is when a satellite camera is formed by two satellites with the goal of the formation to form a telescope that can acquire high-resolution multispectral images of the Earth's surface with the use of two small satellites

instead of one big and more expensive satellite. One of the satellites holds the optical system with lenses and/or mirrors and the other one the detectors (sensors). In our experiment Tango was simulating the holder of the optical system with lenses and/or mirrors while Mango was simulating the holder of detectors.

The experiment was performed in two different versions. In the first version the satellites were flying one after the other in an along-track formation which is preferable as the consumption of propellant is very small. Regarding the imaging types, there are two possibilities of acquiring images. If a linear scanner is used in a sweeping motion, it can cover a larger area. The other type is the “pointing mode” acquisition that can also be used when the same area is imaged several times. In this case a full frame detector that covers a smaller area would be needed.

In the second version of the experiment, the satellites were flying in slightly different orbits (parallel flying – radial and cross-track displacement). The satellites were aligned with predefined target locations on the Earth, including Cape Town (South Africa), Piran (Slovenia) and Punta Arenas (Chile). Depending on the version of the experiment, Mango was driven to an appropriate position as described in the next two Subsections.

4.1. In-track displacement

To obtain a high multispectral resolution and to keep the combined instrument as small as possible both satellites should be placed close to each other, in the range of less than 5 m. With such small distances, high precision formation flying and attitude control is needed. To avoid blurred images when imaging, both systems have to be precisely aligned and kept at a constant relative distance and orientation. The satellites were flown in approximately the same orbit (parallel flying – in-track displacement) - a mirror at an angle of approximately 45 degrees is needed to reflect the beam to the sensors.

In the experiment we have tested the above mentioned configuration - Mango and Tango were positioned in-track at a relative distance of approximately 5 m. The position was kept for two orbits. During these orbits the absolute and relative position and attitude of the satellites were measured. From the obtained data we assessed the stability and capability of the formed instrument for high-resolution imaging. The results showed quite unstable motion of the satellites during both orbits. The left part of Figure 5 shows the degree of change in the viewing direction of Mango body axis. The changes are mainly below 0.1 degrees in all axes but contain major fluctuations that can reach values over 1 degree due to orbit thrusting. This results in a pointing shift of at least approximately 1 cm. The situation with Tango is even worse as the axes deviate more than 20 degrees due to the fact that Tango has only a 3-axis magnetic body control [12].

The relative position of the satellites was maintained with the use of Mango thrusters that regulated satellite motion. During the orbits the relative distance between the satellites changed up to more than 10 cm in all axes (Figure 5 right). The variations are

relatively small but show clear instability. The axis in the flight direction showed the highest stability.

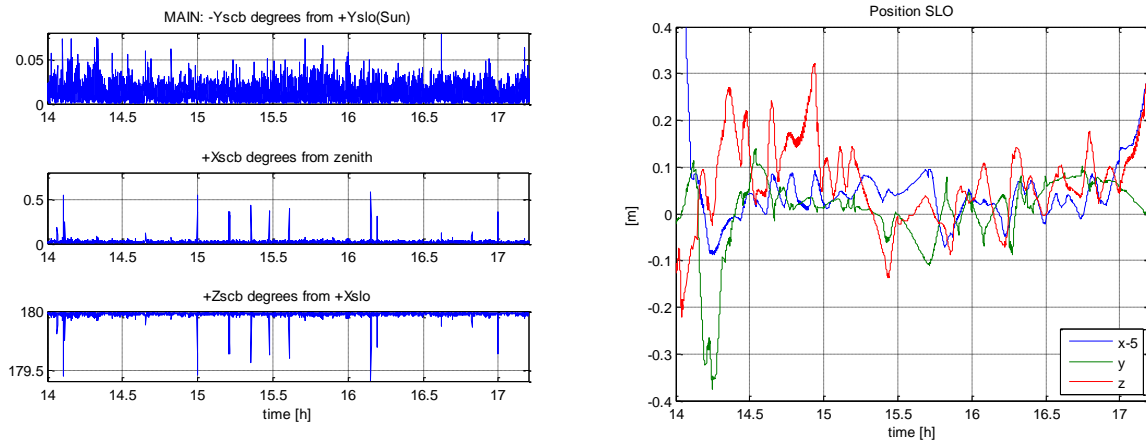


Figure 5: Changes of the Mango's attitude (left) and relative distance variations between the satellites (right) during two consecutive orbits.

4.2. Radial and cross-track displacement

The satellites were flown in slightly different orbits (parallel flying – radial and cross-track displacement). The satellites were aligned with predefined target locations on Earth's surface, including Cape Town (South Africa), Piran (Slovenia) and Punta Arenas (Chile). The experiment was initially planned for July 2011, however, due to delays it was shifted to mid-September 2011 – the time of autumnal equinox. This is not an appropriate time for taking images of the Earth's surface from a dusk-dawn orbit. In addition due to the inclination of the orbit the targets on the southern hemisphere had much better lighting condition than those on the northern, where our preferred area of interest Piran/Portorož (venue of The 4S Symposium 2012), was located.

The evening passage was chosen because the Prisma satellites crossed the equator line 30 minutes before reaching the terminator and could be at the same time in the field of view of Kiruna ground control station while over the target of Piran.

The best lighting conditions for Piran were on the first day of experiments – September 19, 2011. However the weather conditions were not acceptable with total cloud cover over the target area. The best weather forecast was for Wednesday, September 21, 2011 however the trajectory was very unsuitable. The first passage was far eastward of the target – about eastern Black sea, the second one about 10 minutes after the sunset. Despite this fact the decision was taken to go ahead with the experiment on this day and to add a second target – Cape Town where the 62nd International Astronautical Congress was held one month later.

Orbitron was used to determine the approximate time of an appropriate passage. The approximate time and the TLE data of Tango were supplied to a Matlab based satellite simulator, which calculated the closest satellite position with respect to the target. Using the satellite-target vector and desired Mango-Tango distance the relative position of

Mango in the Tango co-ordinate system was calculated and supplied to the STK program for verification. The orientation of Tango was unchanged (the solar panels facing the Sun), while Mango was turned to track the ground target with its DVS camera during the passage.

On September 21, 2011 the experiment included three targets (Piran, Cape Town, Piran) during one orbit. The experiment with Piran as target was repeated next day, however high clouds covered the target area, so only the imaging over the third target – Terra del Fuego with the Strait of Magellan (Punta Arenas) was successful. Figure 6 shows the STK simulated (left first and third) and real (DVS) shots (left second and fourth) of of Tango aligning with Cape Town (left two) and Punta Arenas (right two).

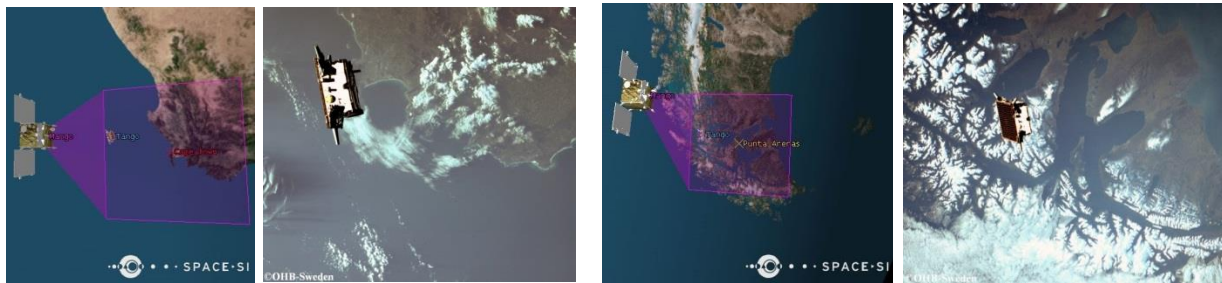


Figure 6. The STK simulated (left first and third) and real (DVS) shots (left second and fourth) of of Tango aligning with Cape Town (left two) and Punta Arenas (right two).

On May 9, 2012 the experiment for aligning the Tango with Piran was repeated and the result is shown in Figure 7 where the sequence of three STK verifications of Matlab calculated data and three DVS shots in 7.5s time intervals is depicted from left to right. In the DCS shots he city of Piran is indicated by red star and the gulf of Trieste can be seen.

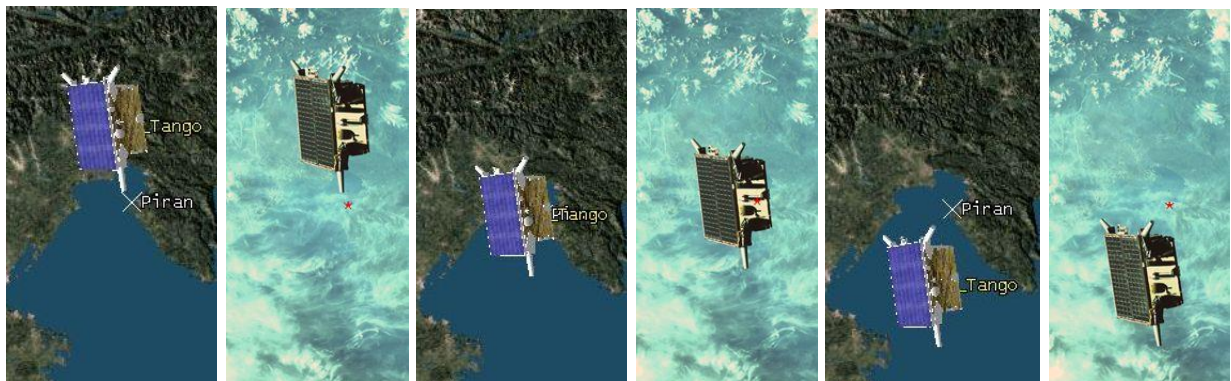


Fig. 7: The sequence of images of Tango aligning with Piran in the background

5.3. Lessons learned

The lesson learned with the In-track formation was that very precise orbit maneuvering and navigation, required for exact focusing (in micrometer scale), cannot be achieved

by the implemented thruster-control and GPS navigation technology. It can be concluded that accuracies in the regulation of relative distances and attitudes are inadequate for a distributed platforms instrument where relative positions and attitude shifts should be kept within millimeters. This is true for both the line scanner and for a full frame camera because the axis instability cannot be accurately predicted. For satisfactory results both satellites would have to use reaction wheels, thrusters with a precise regulation as well as a precise relative navigation system. Relative GPS navigation as used in this experiment is not a suitable choice when millimeter position accuracy is needed.

The experiment of the radial and cross-track displaced instrument remote sensing simulation has shown that the positioning of the satellites in order to align them with predefined targets was satisfactory as demonstrated by attractive pictures despite very unsuitable (for taking images of the Earth's surface) dusk down orbit, autumnal equinox time and bad weather.

5. Critical Evaluation of Formation Flying Models

The last but not the least lesson has been learned by the critical evaluation of formation flying models. The astrodynamical data of the in-flight simulated radar interferometry remote-sensing experiment is used to verify several formation flying models including a nonlinear model, a linear Hill-Clohessy-Wiltshire model, STK models with four propagators (Earth mass point, J2, default HPOP and HPOP with all disturbances) and the hereby originally proposed extension to the Hill-Clohessy-Wiltshire model, a linear model for orbits with small eccentricities (derived by the method of perturbations), which can cope with the phenomenon of eccentricity adequately and mitigates for the shortcomings of the currently widely used model sets. The obtained model is linear with time varying parameters (depending on the target's satellite true anomaly).

5.1. Formation flying models

First formation flying model was the non-linear model based on two-body problem, described by the following set of nonlinear equations

$$\begin{aligned}\ddot{x} - 2\dot{\varphi}_R\dot{y} - \ddot{\varphi}_R y - \dot{\varphi}_R^2 x - \frac{\mu(R+x)}{((R+x)^2+y^2+z^2)^{\frac{3}{2}}} + \frac{\mu}{R^2} + a_x \\ \ddot{y} + 2\dot{\varphi}_R\dot{x} + \ddot{\varphi}_R x - \dot{\varphi}_R^2 y = -\frac{\mu y}{((R+x)^2+y^2+z^2)^{\frac{3}{2}}} + a_y \\ \ddot{z} = -\frac{\mu z}{((R+x)^2+y^2+z^2)^{\frac{3}{2}}} + a_z\end{aligned}\quad (1)$$

where x_n (Radial), y_n (In-track) and z_n (Cross-track) are the coordinates of the main satellite in the target satellite coordinate system (called Radial/In-track/Cross-track – RIC) and a_x , a_y , a_z are the accelerations of the main satellite in the radial, in-track and cross-track direction, respectively. In the above equations R is the distance of the target satellite from Earth mass point, μ the Earth gravitational constant, and φ_R the true

anomaly of the target. The movement of the target satellite is described by the following nonlinear equations:

$$\ddot{R} = R\dot{\phi}_R^2 - \frac{\mu}{R^2} \quad \ddot{\phi}_R = -\frac{2\dot{R}\dot{\phi}_R}{R} \quad (2)$$

These equations include the influence of the eccentricity and nonlinear differential gravitation, however do not include disturbances, such as oblateness of the earth (e.g. J2 coefficient) and third bodies influences. The model is realized within STK as Earth mass point propagator.

Hill-Clohesy-Wiltshire (HCW) model is obtained for close formation flying by the linearization of Equations (1, 2) and by the assumption of a circular orbit ($R = a$, angular acceleration zero), yielding the mean motion $\dot{\phi}_R = n = \sqrt{\frac{\mu}{a^3}}$. It is as follows

$$\begin{aligned} \ddot{x}_c - 2n\dot{y}_c - 3n^2x_c &= a_x \\ \ddot{y}_c + 2n\dot{x}_c &= a_y \\ \ddot{z}_c + n^2z_c &= a_z. \end{aligned} \quad (3)$$

These equations describe the movement of the main satellite with respect to the target satellite for circular orbit and small deviations. For constant accelerations a_x , a_y , and a_z , this system of equations can be solved analytically.

For orbits with small eccentricities a linear model was developed by the method of small deviations (perturbations) [13]. In this case the co-ordinates are expressed as deviations from the HCW model solutions with the eccentricity ε as small parameter

$$\begin{aligned} x(t) &= x_c(t) + \varepsilon x_1(t) \\ y(t) &= y_c(t) + \varepsilon y_1(t) \\ z(t) &= z_c(t) + \varepsilon z_1(t) \end{aligned} \quad (4)$$

The resulting deviation model is

$$\begin{aligned} \ddot{x}_1 - 2n\dot{y}_1 - 3n^2x_1 &= (10n^2x_c + 4n\dot{y}_c)\cos(nt) - 2n^2y_c\sin(nt) \\ \ddot{y}_1 + 2n\dot{x}_1 &= (-4n\dot{x}_c + 4n^2y_c - 3n^2y_c)\cos(nt) \\ \ddot{z}_1 + n^2z_1 &= -3n^2z_c\cos nt. \end{aligned} \quad (5)$$

With the following initial conditions

$$x_1(0) = z_1(0) = 0 \quad y_1(0) = y_0 \quad \dot{x}_1(0) = ny_0 \quad \dot{y}_1(0) = \dot{z}_1(0) = 0 \quad (6)$$

5.1. Evaluation of the models

The experimental data acquired during in-flight simulated radar interferometry propagation were used to evaluate and compare the models with respect to how they capture relative dynamics of the satellites considering different phenomena, such as orbit eccentricity and Earth oblateness. The experimental measurements have been improved by Precise Orbit Determination (POD) [14] to the precision of the relative position of 2 cm, 3D, rms. During this experiment Mango was flown without trajectory

control, the safety box for Mango was set to 10m. In an ideal case (HCW model, zero relative initial velocity) the satellites would fly in constant in-track distance. However the experiment exhibits some periodic motion and a parabolic drift, which are due to an elliptical orbit, nonzero initial conditions and real environment. To eliminate the influence of initial conditions, the models were individually optimized. We believe that the parabolic drift was due to the difference of the drag of both satellites. In order to eliminate it, a constant acceleration in the in-track direction was added to Mango. Initial relative positions, initial relative velocities and a constant in-track acceleration were obtained by means of optimisation.

There was a slight cross-track sinusoidal movement of Mango in Tango's RIC coordinate system with amplitude of 57cm. All models cope with this movement within an error of 16mm which is below the precision of the POD data. So only the Radial/In-track models will be shown here. The optimization was performed in Matlab using the function `fminsearch` with the cost function equal to the average distance between the model response POD the POD data.

Figure 9 represents the projection of the relative Mango orbit into the Tango orbital plane, the radial and the in-track deviations of the model response to the POD data for various models. From presented results it is obvious that there are three groups of models. In the first group there is the simple HCW model (represented in solid green) with the worst cost function and greatest deviations. The first harmonic deviations in this model are the consequence of orbit eccentricity.

In the second group there are the non-linear model (dotted), the STK Earth Mass Point model (dashed) and the newly developed (by the method of perturbations) linear model (solid). All three models are presented in red colour. It should be noted that the non-linear and the STK-EMP model are theoretically identical and that the newly developed linear model is very similar to them due to the small eccentricity of the Prisma orbits (0.004). Second harmonic deviations can be observed, which are due to the oblateness of the Earth. STK J2 and High Precision Orbit Propagator models form the third group. It can be observed that they eliminated the effect of the Earth oblateness.

Obviously the HPOP propagators (default settings and with all disturbances included) do not exhibit any improvement of the model over the J2 model. In all STK models a numerical noise can be observed too. It can be concluded that the newly developed linear model for orbits with small eccentricities can cope with this phenomenon adequately and mitigates for the shortcomings of the currently widely used model sets.

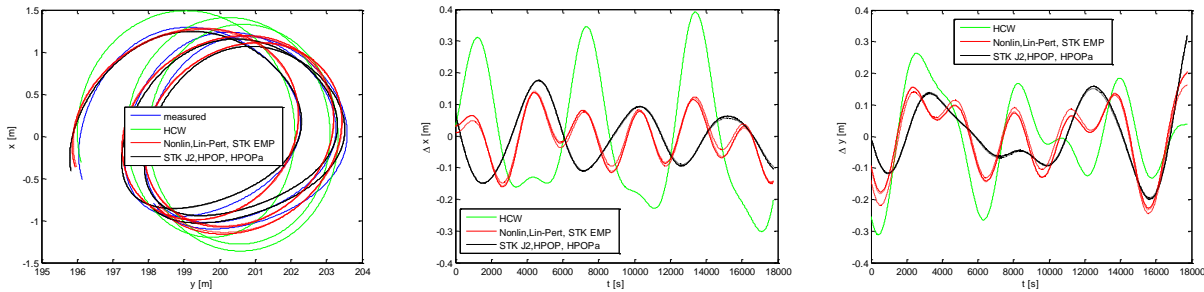


Figure 11. The projection of the relative Mango orbit into the Tango orbital plane (left), radial (left) and in-track (right) deviations of the model response to the POD data for various models

5.3. Lessons learned

Unfortunately raw data from the sensors were not at our disposal due to the preprocessing. The models were fitted to the data from a POD product, which is already the output of a reduced dynamics orbit determination (employing rigorous force models, which however were not known to us). The question arising was, whether our successive model comparison did provide the accuracy of a kind of an orbit determination rather than the true net propagation error of the models, intended to be used for the orbit prediction.

Our intention was not to compare the models with respect to their ability to predict the relative propagation but with the respect to their ability to cope various with phenomena, such as e.g. Earth oblateness etc. If the POD data is obtained by a kind of a Kalman filter (including a model) then the POD data is the best estimate of the real position of the satellites and this is, what is in our interest. Our desire was to fit the responses of the model to the real (relative) position of the satellites, not to fit them to the faulty measurements.

The lesson learned is that while preprocessing significantly reduces the noise, it also introduces some filtering artifacts and due to these artifacts the evaluation of the models becomes extremely difficult. It will be part of our future work.

6. Conclusions

Lessons learned from experiments performed by SPACE-SI and OHB Sweden in September 2011 with Prisma satellites are reviewed. The In flight simulated synthetic aperture radar interferometry remote sensing experiment demonstrated that speed estimation accuracy can reach 0.05 m/s, while in a similar cross-track constellation with similar orbital parameters the vertical accuracy of the digital elevation model production could reach 1 m. The Observation of non-co-operative objects - space debris experiment has proven that space debris, a serious problem in near future, can be identified on the basis of available NORAD TLE data and optically tracked by a narrow (14°) camera. It can also be modelled by using close images taken from various directions under satisfactory illumination conditions. For better metric results the use of

a previously calibrated camera is highly recommended. A collateral outcome of close observation from an orbit, which is encircling the target by its natural motion, were also images with interesting spots on the Earth (Kuwait, Djibouti, Crete) in the background. Here the timing of images was precisely calculated in order to capture both targets simultaneously. The in-flight simulated distributed instrument experiment, where one of the satellites holds the optical system with lenses and/or mirrors and the other one the detectors (sensors), has proven that very precise orbit manoeuvring and navigation, required for exact focusing, cannot be achieved by the implemented thruster-control and GPS navigation technology of Prisma satellites. However the positioning of the satellites in order to align with predefined targets (Piran, Cape Town, Punta Arenas) was satisfactory as demonstrated by the attractive pictures despite very unsuitable (for taking images of the Earth's surface) dusk dawn orbit, the autumnal equinox and extensive cloud coverage over the target area.

Several formation flying models are reviewed, such as nonlinear model and its linearization – the HCW model. An extension of the linear HCW model to orbits with small eccentricities is derived by the method of perturbations. The obtained model is linear with time varying parameters (depending on the target's satellite true anomaly).

The astrodynamic data of the in flight simulated radar interferometry remote-sensing experiment were used to verify several formation flying models including a nonlinear model, a linear Hill-Clohessy-Wiltshire model, STK models with four propagators (Earth mass point, J2, default HPOP and HPOP with all disturbances) and the hereby originally proposed extension to the Hill-Clohessy-Wiltshire model, a linear model for orbits with small eccentricities, which can cope with the phenomenon of eccentricity adequately and mitigates for the shortcomings of the currently widely used model sets. The lesson learned is that while preprocessing significantly reduces the noise, it also introduces some filtering artifacts and due to these artifacts the evaluation of the models becomes extremely difficult.

6. Acknowledgements

The Centre of Excellence for Space Sciences and Technologies SPACE-SI is an operation partly financed by the European Union, European Regional Development Fund and Republic of Slovenia, Ministry of Higher Education, Science and Technology.

7. References

- [1] Persson S., Jacobsson B., Gill E., PRISMA - Demonstration Mission for Advanced Rendezvous and Formation Flying Technologies and Sensors, Proceedings of the 56th International Astronautical Congress (IAC-05-B5.6.B.07), Fukuoka, Japan, October 2005.
- [2] Persson S., Jacobsson B., "PRISMA - Swedish in-orbit test bed for rendezvous and formation flying," Proceedings of the 57th IAC/IAF/IAA (International Astronautical Congress), Valencia, Spain, Oct. 2-6, 2006, IAC-06-D1.2.02

[3] Larsson R., Berge S., Bodin P., Jönsson U., Fuel Efficient Relative Orbit Control Strategies for Formation Flying and Rendezvous within PRISMA, 29th ANNUAL AAS GUIDANCE AND CONTROL CONFERENCE, Colorado February 4-8, 2006.

[4] <http://ohb-sweden.se/Prisma>

[5] Richards J., Remote Sensing with Imaging Radar. Springer, 2009.

[6] Krieger, G.; Moreira, A.; Fiedler, H.; Hajnsek, I.; Werner, M.; Younis, M.; Zink, M.; , "TanDEM-X: A Satellite Formation for High-Resolution SAR Interferometry," Geoscience and Remote Sensing, IEEE Transactions on , vol.45, no.11, pp.3317-3341, Nov. 2007.

[7] Yoon, Y. T., Eineder, M., Yague-Martinez, N. and Montenbruck, O., "TerraSAR-X precise trajectory estimation and quality assessment," IEEE Trans. Geosci. Remote Sens., vol. 47, no. 6, pp. 1859–1868, Jun. 2009.

[8] Romeiser, R. and Thompson, D. R., "Numerical study on the along-track interferometric radar imaging mechanism of oceanic surface currents," IEEE Trans. Geosci. Remote Sens., vol. 38, no. 1, pp. 446–458, Jan. 2000.

[9] Stockburger, Edward. F., Hugh D., Holt Jr, Daniel N. Held, and Robert A. Guarino. "Interferometric moving vehicle imaging apparatus and method." U.S. Patent 5,818,383, issued October 6, 1998.

[10] www.agi.com.

[11] Reigber, C., Xia, Y. Kaufmann, H., Timmen, T., Bodechtel, J. and Frei, M., "Impact of precise orbits on SAR interferometry," in Proc. FRINGE 96 Workshop, Zurich, Switzerland, 1996.

[12] Chasset, C., Berge, S., Bodin, P. and Jakobsson, B., 3-axis Magnetic Control with Multiple Attitude Profile Capabilities in the PRISMA Mission, Space Technology, Vol. 26, Issue 3-4, 2007, pp 137-154.

[13] Matko, D., Rodič, T., Blažič, S., Marsetič, A., Oštir, K., Mušič, G., Teslić, L., Klančar, G., Peljhan, M., Zobavnik, D., Larsson, R., Clacey, E., Swärde, C., Karlsson, T., Validation of astrodynamics formation flying models against SPACE-SI experiments with prisma satellites. V: 26th Annual AIAA/USU Conference on Small Satellites, August 13-16, 2012, Logan, Utah, USA.

[14] D'Amico S., Ardaens J.-S., Larsson R.; Spaceborne Autonomous Formation Flying Experiment on the PRISMA Mission; AIAA Guidance, Navigation, and Control Conference, 8-11 Aug. 2011, Portland, USA (2011). Journal of Guidance, Control and Dynamics (2012, in print). David A. Vallado, Fundamentals of Astrodynamics and Applications (2nd Edition).